Open access • Journal Article • DOI:10.1097/01.SHK.0000168526.97716.F3

The acute inflammatory response in diverse shock states. — Source link

Carson C. Chow, Gilles Clermont, Rukmini Kumar, Claudio Lagoa ...+8 more authors

Institutions: University of Pittsburgh

Published on: 01 Jul 2005 - Shock (Shock)

SHOCK, Vol. 24, No. 1, pp. 74–84, 2005

THE ACUTE INFLAMMATORY RESPONSE IN DIVERSE SHOCK STATES

Carson C. Chow,* Gilles Clermont,† Rukmini Kumar,‡ Claudio Lagoa,§ Zacharia Tawadrous,† David Gallo,§ Binnie Betten,§ John Bartels,‖ Gregory Constantine,* Mitchell P. Fink,† Timothy R. Billiar,§ and Yoram Vodovotz§

**Department of Mathematics, †Department of Critical Care Medicine, ‡Department of Physics and Astronomy, and §Department of Surgery, University of Pittsburgh, Pittsburgh, Pensylvania; and ‖Immunetrics, Inc., Pittsburgh, Pennsylvania*

Received 15 Dec 2004; first review completed 4 Jan 2005; accepted in final form 13 Apr 2005

ABSTRACT—A poorly controlled acute inflammatory response can lead to organ dysfunction and death. Severe systemic inflammation can be induced and perpetuated by diverse insults such as the administration of toxic bacterial products (e.g., endotoxin), traumatic injury, and hemorrhage. Here, we probe whether these varied shock states can be explained by a universal inflammatory system that is initiated through different means and, once initiated, follows a course specified by the cellular and molecular mechanisms of the immune and endocrine systems. To examine this question, we developed a mathematical model incorporating major elements of the acute inflammatory response in C57Bl/6 mice, using input from experimental data. We found that a single model with different initiators including the autonomic system could describe the response to various insults. This model was able to predict a dose range of endotoxin at which mice would die despite having been calibrated only in nonlethal inflammatory paradigms. These results show that the complex biology of inflammation can be modeled and supports the hypothesis that shock states induced by a range of physiologic challenges could arise from a universal response that is differently initiated and modulated.

KEYWORDS—Mathematical modeling, inflammation, shock, organ dysfunction, hemorrhage

INTRODUCTION

Acute systemic inflammation is triggered by both infection and trauma. This response involves a cascade of events mediated by a network of cells and molecules. The process localizes and identifies an insult, strives to eliminate offending agents, and initiates a repair process. If the system functions properly, inflammation eventually abates, and the body returns to equilibrium. However, the inflammatory response can also compromise healthy tissue, further exacerbating inflammation (1, 2) and possibly culminating in organ failure or death (3).

Shock and organ dysfunction are major healthcare problems that afflict victims of both trauma and sepsis. In 1999, a quarter of a million deaths were associated with sepsis in the United States alone (4, 5).

The initial progression of systemic inflammation can have different manifestations depending on how it is triggered, i.e., infection or trauma. However, as it progresses, the resulting shock states and organ dysfunction converge. Thus, in developing treatments and predicting outcome, it is important to ascertain which elements of inflammation are universal and which are specific to the initial insult.

Much has been learned regarding the cellular and molecular mechanisms of the acute inflammatory response. However, except for recombinant human activated protein C (Drotrecogin Alfa [activated]) (6) and low-dose corticosteroids in patients with relative adrenal insufficiency (7), this knowledge has not led to effective therapies for inflammation-induced shock. Many attempted antiinflammatory strategies have failed to improve outcome in large, randomized trials, despite showing promise in animal and early-phase human studies (8).

One reason for this failure may be that inflammation-induced shock is a complex process. The full consequences of modulating single pathways or mediators are difficult to predict from the knowledge of those pathways or mediators in isolation. Additionally, the correct therapy may depend on the exact stage and trajectory of the disease. We suggest that the complexity and diversity of shock states arises from the time-dependent interactions of a unified inflammatory response that is highly sensitive to specific modes of initiation and modulation. We further propose that this complexity might be effectively captured in a mathematical model that incorporates the dynamic interactions of a few key elements of the acute inflammatory response. A mathematical model might likewise provide new insights into the global consequences of manipulating individual components of inflammation. Mathematical modeling is increasingly being used to address biological complexity, in some cases leading to novel predictions (9–13).

We have previously described two mathematical models of inflammation of increasing complexity. The simpler model, consisting solely of a pathogen, a single population of inflammatory cells, and a measure of global tissue damage/dysfunction, could describe both recoverable infection and septic shock (14).

Address reprint requests to Gilles Clermont, MD, MSc, Department of Critical Care Medicine, University of Pittsburgh, Scaife 606B, 3550 Terrace Street, Pittsburgh, PA 15261. E-mail: cler@pitt.edu.

Drs. Chow, Clermont, and Vodovotz are minority shareholders of Immunetrics, Inc. and also provide consultancy services to Immunetrics, Inc. within the terms defined by the University of Pittsburgh policy on conflicts of interest. Drs. Fink and Billiar provide consultancy services to Immunetrics, Inc. John Bartels is an employee of Immunetrics, Inc.

DOI: 10.1097/01.shk.0000168526.97716.f3

A more complex model was used to create simulated populations of septic patients and to simulate a clinical trial of anti-TNF therapy (15). In this paper, we report a further enhancement to our mathematical model of acute inflammation and shock, based on some known underlying cellular and molecular mechanisms of inflammation. Our model represents the simultaneous interactions of several different pathways. Specifically, we show that it can account for the temporal changes in the concentrations of three selected cytokines and nitric oxide by-products in mice, for disparate initial insults involving bacterial lipopolysaccharide (LPS, endotoxin), surgical trauma, and hemorrhage.

MATERIALS AND METHODS

Experimental procedures

Mice—All animal experiments were approved by the Institutional Animal Care and Use Committee of the University of Pittsburgh. The experiments were performed in adherence to the National Institutes of Health Guidelines on the Use of Laboratory Animals. All studies were carried out in C57Bl/6 mice (6–10 weeks old; Charles River Laboratories, Charles River, ME).

Endotoxemia protocol—Mice received either LPS (from *E. coli* O111:B4, 3, 6, or 12 mg/kg intraperitoneally; Sigma Chemical Co., St. Louis, MO) or saline control. At various time points following this injection, the mice (four to eight separate mice per time point) were euthanized, and their sera were obtained for measurement of various analytes (see below). All of the mice survived this high dose of LPS until the final time point (24 h following injection of LPS).

Surgical trauma and hemorrhagic shock protocols—For surgical trauma and hemorrhagic shock treatment, mice were anesthetized, and both femoral arteries were surgically prepared and cannulated. For hemorrhagic shock, the mice were then subjected to withdrawal of blood with a mean arterial pressure (MAP) maintained at 25 mmHg for 2.5 h with continuous monitoring of blood pressure as described previously (16). The normal MAP in mice is approximately 100 mmHg. In the resuscitated hemorrhage groups, the mice were resuscitated over 10 min with their remaining shed blood plus two times the maximal shed blood amount in lactated Ringer solution via the arterial catheter. For trauma, only the surgical preparation was conducted. In some cases, LPS was administered intraperitoneally to mice undergoing hemorrhagic shock. Animals were euthanized by exsanguination, and their serum analyzed as described below.

Analysis of cytokines and NO_2^-/NO_3^-—The following cytokines were measured using commercially available ELISA kits (R&D Systems, Minneapolis, MN): TNF, IL-10, and IL-6. Nitric oxide was measured as NO_2^-/NO_3^- by the nitrate reductase method using a commercially available kit (Cayman Chemical, Ann Arbor, MI) (17). Aspartate aminotransferase (AST) was measured using a commercially available kit (Vitros Chemistry™; Ortho-Clinical Diagnostics, Raritan, NJ) according to manufacturer's instructions.

Mathematical model of acute inflammation

We constructed a mathematical model of acute inflammation that incorporates key cellular and molecular components of the acute inflammatory response (see Results, Table 1, and Appendix). The mathematical model consists of a system of 15 ordinary differential equations that describe the time course of these components. Included in the model equations are two systemic variables that represent mean arterial blood pressure and global tissue dysfunction and damage. ''Global tissue damage/dysfunction'' describes the overall health of the organism because the hallmark of the pathology accompanying sepsis and hemorrhagic shock is the eventual, sequential failure of multiple organs. Given the complexity of simulating individual organs, we approximated this process by treating it as a gradual, ongoing process occurring in the whole body and driven by inflammation. Thus, unrecoverable tissue damage/dysfunction served as a surrogate for death, whereas damage/dysfunction that tended to return to baseline over a several-day period was a proxy for survival. In the model, pathogen-derived products, trauma, and hemorrhage are initiators of inflammation. (We note that hemorrhage is caused by injury that disrupts the integrity of blood vessels, and thus the two processes must be included in an accurate simulation).

Each equation was constructed from known interactions among model components as documented in the existing scientific literature. In deriving the mathematical model, we balanced biological realism with simplicity. Our goal was to find a fixed set of parameters that would qualitatively reproduce many known scenarios of inflammation found in the literature, correctly describe our data, and serve as a platform for eventually testing novel predictions experimentally.

The model and parameters were specified in three stages. In the preliminary stage, the model was constructed so it could reproduce qualitatively several different scenarios reported in the literature. In this stage, direct values of parameters such as cytokine half-lives were used when available. In the second stage, the model was matched to our experimental data by adjusting some of the parameters using our knowledge of the biological mechanisms together with the dynamics of the model to attain desired time course shapes. In the third stage, the parameters were optimized using a stochastic gradient descent algorithm that was implemented in software of Immunetrics, Inc. (Pittsburgh, PA).

The units of all the quantities in the model were specified so that for the experimental protocols tested they ranged from zero to one. This was done for computational convenience and has no implications for the underlying biology.

TABLE 1. **Dynamic variables of the mathematical model**

Model component	Comment
Lipopolysaccharide (endotoxin, LPS)	Immunostimulant derived from gram-negative bacteria or administered exogenously
Resting neutrophils (N_R)	Renewable pool of local and circulating neutrophils susceptible to activation
Activated neutrophils (N_A)	Pool of local and circulating activated triggered by LPS, TNF, IL-6, and tissue dysfunction
Resting macrophage (M_R)	Circulating monocyte or local macrophages that act as a cellular pool for activated macrophages. The total count of resting monocyte/macrophages can increase in proportion to the total inflammatory activity
Activated macrophages (M_A)	Activation triggered by LPS, TNF, IL-6, tissue trauma, and tissue dysfunction. Activation is down-regulated by antiinflammatory cytokines
Constitutive nitric oxide synthase (eNOS)	Normally participates in blood pressure homeostasis. Activity is increased by antiinflammatory cytokines and decreased by LPS, TNF, and trauma
Inducible nitric oxide synthase (iNOSd, iNOS)	Increased by LPS and TNF in activated neutrophils and macrophages. Decreased by antiinflammatory cytokines (iNOSd is a precursor to iNOS)
NO_2^-/NO_3^- (NO3)	Stable reaction products of nitric oxide; related to the intensity of the local production of nitric oxide by iNOS and eNOS
TNF	A major early proinflammatory cytokine secreted mainly by activated macrophages but also by activated neutrophils
IL-10	An early antiinflammatory cytokine whose synthesis is triggered by proinflammatory stimuli, antagonizes TNF and iNOS via TNF-dependent and TNF-independent pathways
IL-6	A proinflammatory cytokine with additional antiinflammatory effects
Adrenergic inhibitory activity (CA)	Represents inhibitory activity of the adrenergic system on the production of TNF and IL-6
IL-12	Secreted by activated macrophages in the presence of TNF or IL-6, this cytokine limits the activity of IL-10
Blood pressure (BP)	Homeostasis depends on iNOS and eNOS activity. Blood pressure can be artificially manipulated
Tissue damage (D)	Can be caused by direct trauma, hypotension, or the action of proinflammatory cytokines. Nitric oxide is tissue-protective

However, to compare with experimental data, it was necessary to rescale the model outputs to experimental units by selecting optimal rescaling factors when comparing to data. These factors are specified for only the four quantities for which experimental data were available and convert the arbitrary units into true units. The final parameter set in the Appendix is expressed in arbitrary units for the concentrations and in hours for time.

Comparison to experimental data

The model was calibrated to experimental data sets from five scenarios of inflammation: LPS intraperitoneal injection at 3 mg/kg, 6 mg/kg, and 12 mg/kg; surgical trauma consisting of the insertion of cannulae without further intervention; surgical trauma plus hemorrhage, with procedures as described above. Four analytes—TNF, IL-10, IL-6, and stable reaction products of NO (NO_2^-/NO_3^-)—were measured in all scenarios. These analytes were chosen because they represent a diverse selection of the main responders of the early inflammatory response and are produced on a rapid (TNF, IL-10), intermediate (IL-6), and slow (NO_2^-/NO_3^-) time scale. As we will show, even with this limited data set, the relevant biological mechanisms and the mathematical model are constrained (18, 19). The statistical analysis was performed with the S-Plus statistical and programming package (Statistical Sciences, Inc., Seattle, WA).

Model prediction

We wished to evaluate whether the model could predict a behavior not contained in the training data. We therefore assessed the prediction to a range of endotoxin boluses up to 30 mg/kg, which, from existing literature data, should be lethal (18, 20, 21).

RESULTS

Differences in the kinetics of cytokine and NO production in mouse endotoxemia, trauma, and hemorrhage

Trauma and hemorrhagic shock cause many of the same qualitative inflammatory consequences as endotoxemia, though with different kinetics and magnitude (22). Normal, non-manipulated mice had low levels of cytokines in their serum (data not shown). Surgical trauma alone resulted in elevated circulating levels of the measured cytokines (Fig. 1). In trauma (Fig. 1D), hemorrhagic shock (Fig. 2D), and endotoxemia (Figs. 3D, 4D, and 5D), NO_2^-/NO_3^- levels first decrease and then rise (though the levels of NO_2^-/NO_3^- rise to a much higher peak in endotoxemia). We also note that there is a delay of approximately 2 h before the cytokines respond. The absolute and relative peak levels differ significantly between trauma (Fig. 1) and endotoxemia. Compared with endotoxemia at 3 mg/kg, TNF peak level in trauma is approximately 20 to 40 times lower, IL-6 is approximately 7 times lower, and IL-10 levels are slightly higher. TNF also has a secondary peak at 24 h in trauma. When surgery is followed by hemorrhage, animals had higher peak levels of TNF (Fig. 4A) and IL-6 (Fig. 4C), but similar or slightly higher levels of IL-10 (Fig. 4B) as compared with trauma alone. NO_2^-/NO_3^- has approximately the same form (Fig. 4D). We note that the experimental spread in the data is very large near the peaks. Although the data exhibit large variability at these points, the timing of these peaks is quite predictable.

Generation of a mathematical model of acute inflammation

The dynamics of the measured analytes for these three experimental paradigms exhibit significant differences, although they also share qualitative similarity (2). We propose that the observed differences in the inflammatory responses are caused by differences in the initiating insult: pathogen-derived products versus tissue trauma and/or blood loss. We further propose that, once set in motion, the inflammatory response will follow a path determined by universal physiological mechanisms. For example, it has been recently appreciated that "alarm/danger" molecules such as HMGB1 or HSP-70, thought initially to participate only in the response to pathogens (23), are also important in the process of inflammation induced by sterile means (e.g., trauma) (24). This new paradigm suggests that the host is more concerned with damage or change in the *status quo* than with "foreignness." This response also appears to share receptors: recent articles have implicated TLR4 in the response to sterile inflammation induced by endogenous ligands presumably released from damaged/dysfunctional tissue (for example, in the setting of ischemia/reperfusion injury) (25).

To support our hypotheses, we constructed a mathematical model that incorporates known physiological interactions between the various elements of the immune system. The model structure and parameters are given in the Appendix, and the output of this model in the settings of endotoxemia and trauma/hemorrhage are depicted as solid lines overlying the actual data in the figures. We discuss the statistical analysis of how well the model accounts for the data in the following section.

In the model, neutrophils and macrophages are activated directly by bacterial LPS or indirectly by various stimuli elicited systemically on trauma and hemorrhage. Although not included explicitly in our model, early effects such as mast cell degranulation and complement activation (1) are incorporated

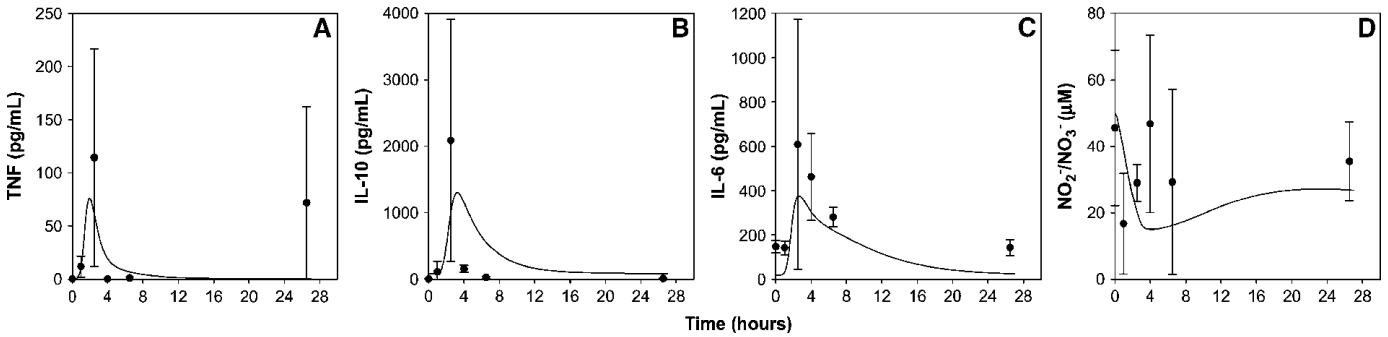

FIG. 1. **Experimental data and model predictions for surgery-induced inflammation**. Mice (3–6 separate mice per time point) were subjected to surgical trauma alone. Animals were euthanized by exsanguination 0, 1.5, or 4 h after surgery. At various time points following this treatment, the mice (3–6 separate mice per time point) were euthanized, and their plasma obtained for analysis of cytokines: TNF (A), IL-10 (B), IL-6 (C), and NO_2^-/NO_3^- (D). Symbols represent values from individual mice; solid lines represent model predictions.

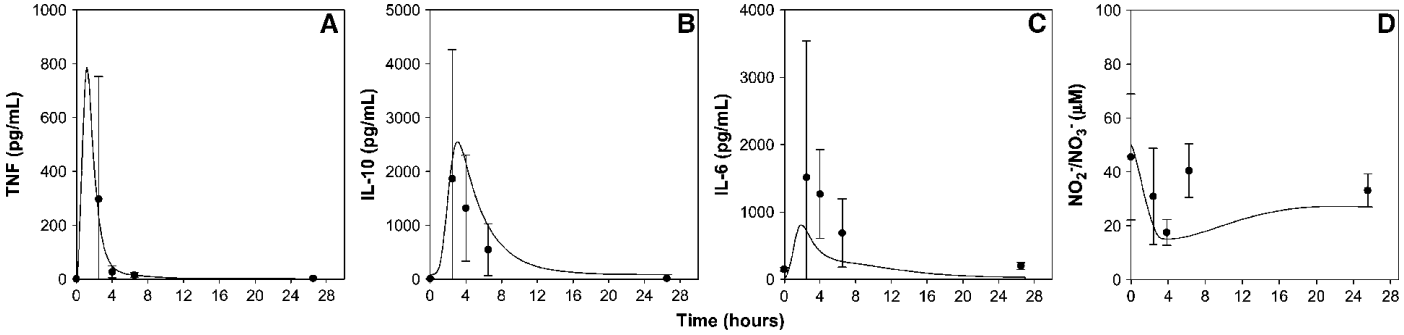

FIG. 2. **Experimental data and model predictions for surgery/hemorrhage-induced inflammation**. Mice (3–6 separate mice per time point) were subjected to combined surgical trauma and hemorrhagic shock. Animals were euthanized by exsanguination 0, 1.5, or 4 h after resuscitation. All analytes were measured as described in Figure 1. Symbols represent values from individual mice; solid lines represent model predictions.

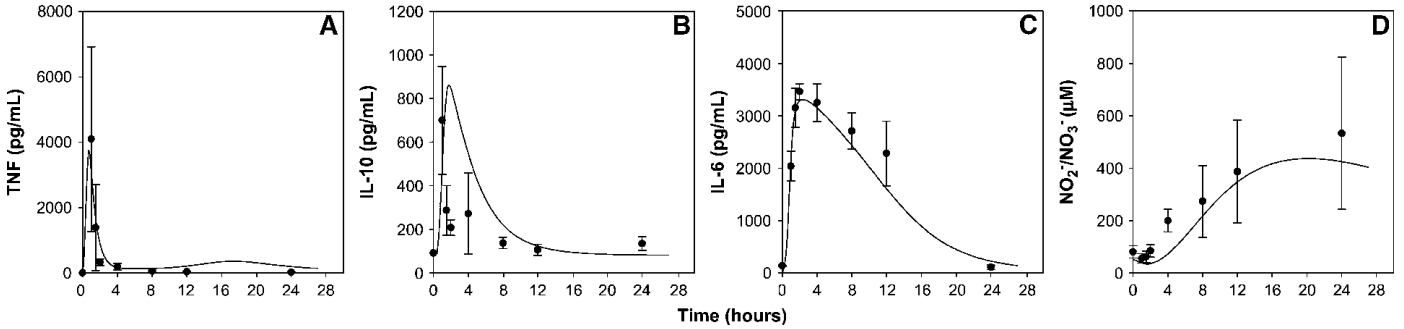

FIG. 3. **Experimental data and model predictions for endotoxemia (3 mg/kg LPS)-induced inflammation**. Mice received either 3 mg/kg LPS or saline control. At various time points following this injection, all analytes were measured as described in Figure 1. Symbols represent values from individual mice; solid lines represent model predictions.

implicitly in the dynamics of our LPS and cytokine variables. These stimuli, including LPS, enter the systemic circulation quickly and activate circulating monocytes and neutrophils (18). Activated neutrophils also reach compromised tissue by migrating along a chemoattractant gradient (26).

Once activated, macrophages and neutrophils produce and secrete effectors that activate these same cells and also other cells, such as endothelial cells. Proinflammatory cytokines—tumor necrosis factor (TNF), interleukin (IL)-6, and IL-12 in our mathematical model—promote immune cell activation and proinflammatory cytokine production (27). The concurrent production of antiinflammatory cytokines counterbalances the actions of proinflammatory cytokines. In an ideal situation, these antiinflammatory agents serve to restore homeostasis. However, when overproduced, they may lead to detrimental immunosuppression (28–30).

Our model includes a fast-acting antiinflammatory cytokine, IL-10, and a slower-acting antiinflammatory activity encompassing active transforming growth factor-β1 (TGF-β1), soluble receptors for proinflammatory cytokines, and cortisol. We note that although activated TGF-β1 has a lifetime of only a few minutes, latent TGF-β1 is ubiquitous (31) and can be activated either directly or indirectly by other slower agents such as IL-6 or NO (32–34).

Proinflammatory cytokines also induce macrophages and neutrophils to produce free radicals. In our model, inducible NO synthase (iNOS)-derived NO is directly toxic to bacteria and indirectly to host tissue (35–37). Although the actions of superoxide (O_2^-) and other oxidative mechanisms (37) do not appear explicitly in the model, their activity is accounted for implicitly through the proinflammatory agents. In the model, the actions of these products that can cause direct tissue dysfunction or damage are subsumed by the action of each cytokine directly. The induced damage can incite more inflammation by activating macrophages and neutrophils (38). However, NO can also protect tissue from damage induced by shock (39–41) even though overproduction of this free radical causes hypotension (36). Proinflammatory cytokines also reduce the expression of endothelial nitric oxide synthase (eNOS), thereby increasing tissue dysfunction (42).

In endotoxemia, the model assumes that LPS enters the bloodstream and incites a system-wide response (43). Lipopolysaccharide is cleared in approximately 1 h (44, 45). Circulating neutrophils are activated directly and produce TNF (46) and IL-10 (47–49). The newly produced TNF combines with LPS to activate macrophages that then secrete TNF, IL-6, IL-12, and IL-10 (50). Activated neutrophils, macrophages, and endothelial cells produce NO through iNOS (51). The model assumes that locally produced NO is eventually detected as the measured serum end products NO_2^-/NO_3^-, and this process depends on the differential induction of eNOS and iNOS in various organs over time (52, 53). In order for TNF to rise and

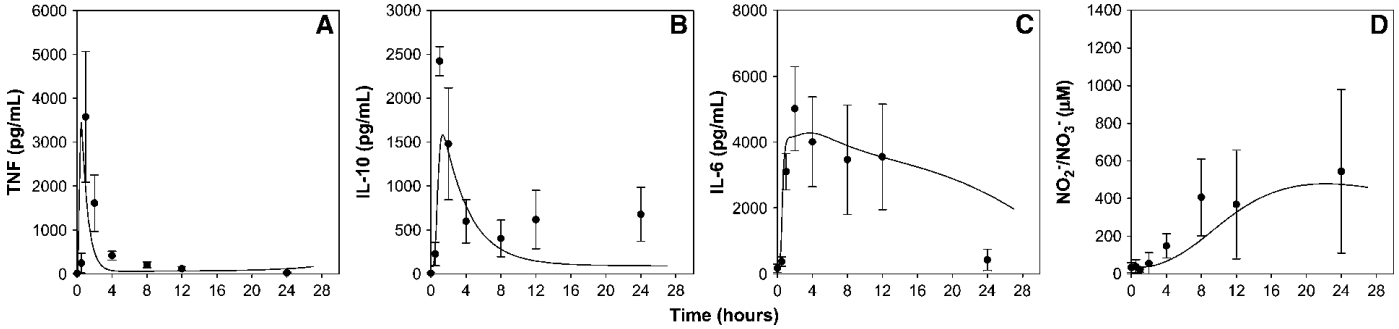

FIG. 4. **Experimental data and model predictions for endotoxemia (6 mg/kg LPS)-induced inflammation**. Mice received either 6 mg/kg LPS or saline control. At various time points following this injection, the mice (3–8 separate mice per time point) were euthanized, and their plasma obtained for analysis of cytokines as in Figure 1. Symbols represent values from individual mice; solid lines represent model predictions.

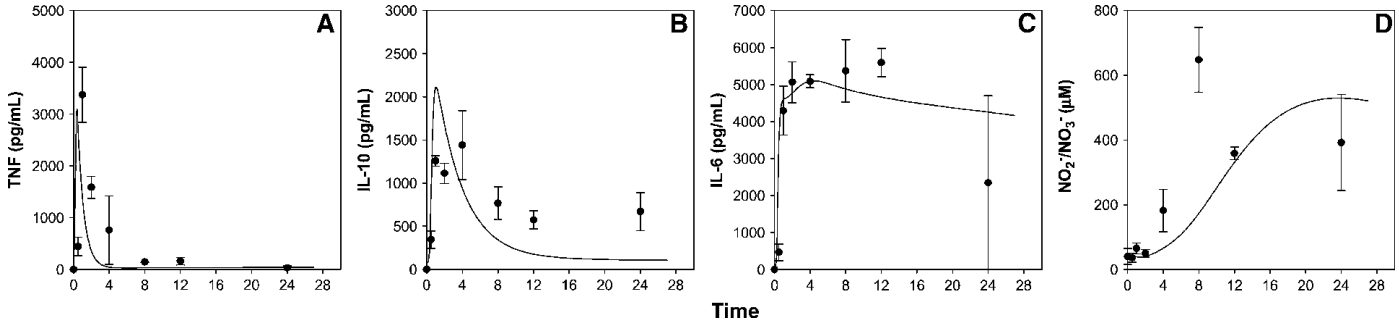

FIG. 5. **Experimental data and model predictions for endotoxemia (12 mg/kg LPS)-induced inflammation**. Mice received either 6 mg/kg LPS or saline control. At various time points following this injection, the mice (3–8 separate mice per time point) were euthanized, and their plasma obtained for analysis of cytokines as in Figure 1. Symbols represent values from individual mice; solid lines represent model predictions.

fall within a few hours as it does in Figure 1, the model required an inhibitory agent to suppress TNF production; this was accounted for by IL-10 (54, 55) and other slow antiinflammatory cytokines including IL-6 (56). Previous work has indicated that IL-6 may exert both pro- and antiinflammatory properties (57). We believe this antiinflammatory action could be mediated by inducing or activating TGF-β1 (32) on the surface of neutrophils and macrophages, as has been shown for cytokines such as interferon-γ (58). To account for the saturation of IL-6 for LPS levels beyond 6 mg/kg (Fig. 2; see also Fig. 5) in the model, we suggest that IL-6 also can act as an antiinflammatory cytokine and inhibit production of itself (59). IL-10 is inhibited by IL-12 (55) and stimulated by TGF-β1 (60), which can come from various sources.

The response to trauma (Fig. 1) exhibits a different time course from endotoxemia (Figs. 3, 4, and 5). To account for these differences in the model, we assume that localized trauma first induces platelets to release TGF-β1 (31), which then chemoattracts circulating neutrophils to the site of injury (61–63). Simultaneously, elements associated with trauma and dysfunctional and/or damaged tissue, possibly HMG-B1 (64), are released and activate the neutrophils when they arrive. The trauma-induced products combine with TNF to activate local macrophages to produce IL-6 and IL-10. To achieve the massive release of IL-10 in comparison to IL-6 and TNF in the model, we assume that catecholamine release by the autonomic nervous system (65) induces production of IL-10 by macrophages (66, 67). Catecholamines also down-regulate production of TNF and IL-6 (68, 69). We also assumed that trauma causes a severe drop in eNOS (or eNOS-derived NO, e.g., by the rapid reduction in availability of l-arginine) (70) to account for the dip in NO_2^-/NO_3^-; it is known that trauma patients exhibit reduced systemic NO_2^-/NO_3^- as compared with uninjured controls (71, 72). A similar drop in eNOS activity or expression also occurs in endotoxemia (73–76).

The model assumes that blood loss in hemorrhage causes some tissue damage as well as directly contributing to neutrophil and macrophage activation (22). This causes a greater release of TNF, which in turn induces higher IL-10 and IL-6 release. The model output suggests that an increase in TNF and IL-6 will be accompanied by an increase in IL-10, though the spread in the data is too large to corroborate this prediction.

Statistical assessment of the model in comparison to the data

Across all scenarios, using all the data points, we obtain a correlation coefficient of 0.81 between the data and the model. Because the scatter of the data is large, trimming outliers seems reasonable. Eliminating 1% of outliers raises the correlation coefficient to 0.86, and a correlation coefficient of 0.90 is obtained by trimming 3% of the outliers. A formal test that the correlation coefficient is zero, versus the alternative that it is

greater that zero, yields a P value <0.0001, with an associated z-value of 38.1, indicating a strong positive dependence between the data and the model.

The correlation coefficients for the four separate data curves in the five scenarios as shown in Figures 1–5 are presented in the Appendix. This analysis indicates that although the model seems to capture the entire data set well, it does not capture the behavior of individual analytes uniformly well in all five scenarios.

Qualitative assessment of the model

We sought to examine the qualitative behavior of our model, in reference to published studies of inflammation in the setting of endotoxemia and/or trauma. We used this process as a form of quality control in the quantitative fitting process of a given iteration of the model, requiring that a given iteration of the model exhibit qualitatively correct behavior across all the scenarios depicted in Table 2. We chose these scenarios as the qualitative test set because those published studies contained information of relevance to the analytes whose time courses are the core of our model.

Prediction of lethal endotoxemia

When subjected to simulated endotoxin loads exceeding 9 mg/kg, the model predicts persistent high levels of IL-6 and high levels of damage (Fig. 6). In fact, the model predicts that cumulative damage will grow rapidly and fail to resolve within the first 24 h with doses exceeding 12 mg/kg. It appears that predicted cytokine levels have reached a plateau at about that dose, with limited increment with higher doses. The small differences in peak cytokine levels we observed between 6 mg/kg and 12 mg/kg support this observation (saturation at or around 15 mg/kg was not built in the model). We would therefore predict that levels as low as 9 mg/kg could be lethal in many animals if not euthanized at 24 h. Indeed, several animals are quite sick at the time of euthanasia. This concurs with the report by Wakatana of an LD_{10} of 10 mg/kg and LD_{90} of 30 mg/kg at 24 h (20). Of note, others reported significantly lower LD_{100} doses in C57/BL6 mice (21). Our own data yielded a LD_{80} of 17 mg/kg (unpublished results).

DISCUSSION

The acute inflammatory response to infection and trauma is highly complex, with many levels of feedback. As a result, the manipulation of a single pathway may lead to unpredictable results. We suggest it is necessary to examine the global response of all the participating cytokines and immune cells simultaneously over several hours or days. Only then can successful therapies be developed systematically (11, 77–80).

Mathematical modeling can provide such a global framework (1, 77, 79, 81). Our model is based on differential equations that represent the dynamics of the mean value of cytokines and cell levels along with variables for blood pressure and global tissue damage/dysfunction. The equations are derivable from physiological interactions using standard principles of mass-action kinetics (82), and the simulated levels can be compared directly to data. This contrasts with our prior work, which presented simpler models of the innate response to an infectious agent without calibration to prospective data (14, 15). The present manuscript describes a continuation of this effort, with the attempt to calibrate the model to actual data; we hope in the future to integrate several more components of the inflammation response. The current model is a very incomplete representation of all the processes of inflammation. However, we believe that it captures many of the main features of acute inflammation and can give new insights into the complex interactions of the process. Moreover, we note that although we used very different modeling strategies and underlying assumptions and elements as compared with other investigators who are simulating acute inflammation (83, 84), our models have often concurred (79).

Though a single mathematical model was able to encompass the dynamics of acute inflammation induced by diverse insults (represented as different starting conditions for our simulations), we found several inconsistencies between the output of the model and our experimental data. For example, we were unable to satisfactorily account for the rise in TNF at 24 h in our model in surgical trauma. Interestingly, we do not see a rise in TNF at 24 h in the trauma/hemorrhage data as we did in trauma alone. This discrepancy probably signifies that the model fails to account for a biological mechanism that is of particular relevance in the interaction of shock and hemorrhage. For example, a possible explanation for this observed discrepancy is that the increase in TNF and IL-6 induces a larger, delayed antiinflammatory response that suppresses TNF later. Therefore, such discrepancies stimulate additional data acquisition to support the existence of mechanisms, either by refining the search for existing data or by guiding the collection of new data. Integration of these mechanisms, in turn, will lead to more accurate models. The process of modeling complex systems, where not all fundamental behaviors and interactions are well understood, is therefore inherently iterative.

TABLE 2. **Qualitative scenarios used in calibration of the mathematical model of inflammation**

Animal	Model	Expected results	References
Mice	Intraperitoneal endotoxin challenge	Increased levels of TNF, IL-6, NO, cardiovascular collapse	(91)
Rats	Intraperitoneal endotoxin challenge (5-100 ug/kg)	Circulatory endotoxin within 15 minutes, 30-90 minutes to IL-6	(92)
Mice	Endotoxin challenge in TNF deficiency	Resistance to endotoxin induced inflammation, increase levels of IL-6.	(93–97)
Mice	Endotoxin challenge in IL-6 deficiency	TNF-α expression is much higher than in wild type animals. In localized tissue damage TGF-β1 and IL-10 are increased.	(98–106)
Mice	Endotoxin challenge and hemorrhagic shock in Nitric Oxide Synthase deficiency.	Decreased hypotension initially, more organ dysfunction, no change in prognosis with endotoxin, decrease cellular recruitment. Lower inflammation in hemorrhagic shock.	(16,107–115)

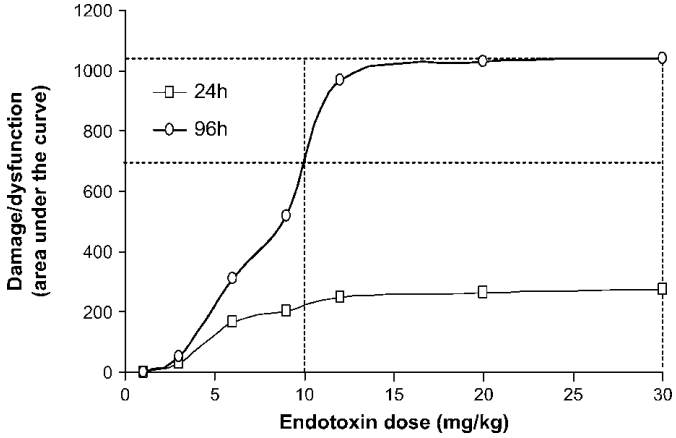

FIG. 6. **Prediction of late damage and mortality following LPS administration**. The model predicted a large increase of total damage/dysfunction at 24 and 96 h at doses of LPS exceeding 9 mg/kg. Open circles and squares represent doses at which the simulations were conducted. The proportion of damage/dysfunction sustained after 24 h is particularly noticeable at higher doses. This suggests that mortality could be associated with the persistence of damage/dysfunction. LD_{10} and LD_{90} doses as reported by Wakahara et al. are projected on the x-axis as dotted lines (20). Total damage seems to plateau at doses exceeding 15 mg/kg. A similar response is seen in the area under the IL-6 curve (data not shown).

We note that agent-based models of systemic inflammation have also been developed (79, 83). In these methods, discrete ''agents'' representing cells and cytokines interact through a set of fixed rules on a spatial grid, with various probabilities of a given interaction taking place. These methods are useful when the participating elements have large amounts of heterogeneity and when they have many internal states that affect their interactions with other elements. Equation-based models like the one we have created are more applicable in settings where the overall behavior of a given variable is sought (i.e., the concentration of a given cytokine in the blood, or the cumulative behavior of neutrophils). We feel that both approaches have merits, and methods incorporating both approaches may be useful in the future (79).

We hypothesize that the acute inflammatory response to diverse insults such as endotoxemia, trauma, and hemorrhagic shock are different manifestations of a universal system. We have attempted to demonstrate this possibility with mathematical modeling. Additionally, our hypothesis is supported by large epidemiologic studies, which indicate that physiological changes, organ failure rates, and survival are similar among patients with infectious and noninfectious causes of acute inflammation (85, 86).

Our model is a biologically based, dynamical simulation. As such, it differs from statistical models based on studies in large patient populations, which seek correlations among various factors (e.g., vital signs and laboratory values) and outcomes (87). Statistical models have demonstrated conclusively that circulating levels of cytokines such as IL-6 correlate with outcome in septic patients (88) and have been successful in understanding average population outcomes. However, these statistical models are mostly descriptive, making limited use of biological mechanisms. Consequently they are unable to provide causal inference and are unreliable to predict outcome of individuals (89).

In conclusion, we have developed this mathematical model with a goal of assisting the rational design of therapies directed against the inflammatory consequences of infection and trauma, the current treatment of which is largely supportive (antibiotics, vasopressors, or mechanical ventilation) (90). Despite suffering from several limitations (a limited subset of inflammatory interactions, the use of mass action kinetics, calibration to circulating but not local levels of cytokines, limited data, and lack of serial measurements in single animals), the model can simulate certain disease scenarios qualitatively as well as simulating the time course of cytokine levels in three distinct paradigms of inflammation in mice. We are in the process of addressing these limitations in various ways. For example, though we did not measure Po_2 and lactate in the studies described in this manuscript, we have an initiated animal studies and inflammation-modeling efforts in the setting of irreversible hemorrhagic shock. In the course of those studies, we are obtaining Po_2, Pco_2, and other measurements and attempting to incorporate these measurements into our damage/dysfunction equation. Extending this mathematical model, with validation in humans, may lead to the *in silico* development of novel therapeutic approaches and real-time diagnostics.

ACKNOWLEDGMENTS

The authors would like to acknowledge funding for this project from Launchcyte, LLC (Y.V., G.C.); Pittsburgh Lifesciences Greenhouse (Y.V.); NIGMS (grants No. R01-GM67240 [G.C., C.C.] and P50-GM53789 [T.R.B., M.P.F., Y.V., G.C.]); and NIAID (grant No. R41 AI52916 [Y.V.]).

REFERENCES

1. Nathan C: Points of control in inflammation. *Nature* 420:846–852, 2002.
2. Jarrar D, Chaudry IH, Wang P: Organ dysfunction following hemorrhage and sepsis: mechanisms and therapeutic approaches. *Int J Mol Med* 4:575–583, 1999.
3. Marshall JC: Inflammation, coagulopathy, and the pathogenesis of multiple organ dysfunction syndrome. *Crit Care Med* 29:S99–S106, 2001.
4. Carrico CJ: 1993 Presidential address, American Association for the Surgery of Trauma: it's time to drain the swamp. *J Trauma* 37:532–537, 1994.
5. Angus DC, Linde-Zwirble WT, Lidicker J, Clermont G, Carcillo J, Pinsky MR: Epidemiology of severe sepsis in the United States: analysis of incidence, outcome, and associated costs of care. *Crit Care Med* 29:1303–1310, 2001.
6. Bernard GR, Vincent JL, Laterre PF, LaRosa SP, Dhainaut JF, Lopez-Rodriguez A, Steingrub JS, Garber GE, Helterbrand JD, Ely EW, Fisher CJ Jr, and the PROWESS Study Group: Efficacy and safety of recombinant human activated protein C for severe sepsis. *N Engl J Med* 344:699–709, 2001.
7. Annane D, Sebille V, Charpentier C, Bollaert PE, Francois B, Korach JM, Capellier G, Cohen Y, Azoulay E, Troche G, Chaumet-Riffaut P, Bellissant E: Effect of treatment with low doses of hydrocortisone and fludrocortisone on mortality in patients with septic shock. *JAMA* 288:862–871, 2002.
8. Bone RC: Why sepsis trials fail. *JAMA* 276:565–566, 1996.
9. Kitano H: Systems biology: a brief overview. *Science* 295:1662–1664, 2002.
10. An G: Agent-based computer simulation and sirs: building a bridge between basic science and clinical trials. *Shock* 16:266–273, 2001.
11. Buchman TG: The community of the self. *Nature* 420:246–251, 2002.
12. Hoffmann A, Levchenko A, Scott ML, Baltimore D: The IkappaB-NF-kappaB signaling module: temporal control and selective gene activation. *Science* 298:1241–1245, 2002.
13. Vodovotz Y, Kim P, Bagci EZ, Ermentrout GB, Chow CC, Bahar I, Billiar TR: Inflammatory modulation of hepatocyte apoptosis by nitric oxide: *in vivo, in vitro*, and *in silico* studies. *Curr Mol Med* 4:753–762, 2004.
14. Kumar R, Clermont G, Vodovotz Y, Chow CC: The dynamics of acute inflammation. *J Theor Biol* 230:145–155, 2004.
15. Clermont G, Bartels J, Kumar R, Constantine G, Vodovotz Y, Chow C: *In silico* design of clinical trials: a method coming of age. *Crit Care Med* 32:2061–2070, 2004.

16. Hierholzer C, Harbrecht B, Menezes JM, Kane J, MacMicking J, Nathan CF, Peitzman AB, Billiar TR, Tweardy DJ: Essential role of induced nitric oxide in the initiation of the inflammatory response after hemorrhagic shock. *J Exp Med* 187:917–928, 1998.
17. Collins J, Vodovotz Y, Billiar TR: Biology of nitric oxide: measurement, modulation, and models. In Souba W, Wilmore D, (eds.): *Surgical Research*. San Diego: Academic Press, 2001, pp 949–969.
18. Parker SJ, Watkins PE: Experimental models of gram-negative sepsis. *Br J Surg* 88:22–30, 2001.
19. Beutler BA, Milsark IW, Cerami A: Cachectin/tumor necrosis factor: production, distribution, and metabolic fate in vivo. *J Immunol* 135:3972–3977, 1985.
20. Wakahara K, Kobayashi H, Yagyu T, Matsuzaki H, Kondo T, Kurita N, Sekino H, Inagaki K, Suzuki M, Kanayama N, Terao T: Bikunin suppresses lipopolysaccharide-induced lethality through down-regulation of tumor necrosis factor-alpha and interleukin-1 beta in macrophages. *J Infect Dis* 191:930–938, 2005.
21. Purswani MU, Eckert SJ, Arora HK, Noel GJ: Effect of ciprofloxacin on lethal and sublethal challenge with endotoxin and on early cytokine responses in a murine in vivo model. *J Antimicrob Chemother* 50:51–58, 2002.
22. Peitzman AB, Billiar TR, Harbrecht BG, Kelly E, Udekwu AO, Simmons RL: Hemorrhagic shock. *Curr Probl Surg* 32:925–1002, 1995.
23. Medzhitov R, Janeway CJ: Innate immunity. *N Engl J Med* 343:338–344, 2000.
24. Matzinger P: The danger model: a renewed sense of self. *Science* 296:301–305, 2002.
25. Tsan MF, Gao B: Endogenous ligands of Toll-like receptors. *J Leukoc Biol* 76:514–519, 2004.
26. Bellingan G: Inflammatory cell activation in sepsis. *Br Med Bull* 55:12–29, 1999.
27. Freeman BD, Natanson C: Anti-inflammatory therapies in sepsis and septic shock. *Expert Opin Investig Drugs* 9:1651–1663, 2000.
28. Volk HD, Reinke P, Docke WD: Clinical aspects: from systemic inflammation to ''immunoparalysis.'' *Chem Immunol* 74:162–177, 2000.
29. Bone RC: Immunologic dissonance: a continuing evolution in our understanding of the systemic inflammatory response syndrome (SIRS) and the multiple organ dysfunction syndrome (MODS). *Ann Intern Med* 125:680–687, 1996.
30. Pinsky MR: Sepsis: a pro- and anti-inflammatory disequilibrium syndrome. *Contrib Nephrol* 132:354–366, 2001.
31. Roberts AB, Sporn MB. Transforming growth factor-b. In Clark RAF (ed.): *The Molecular and Cellular Biology of Wound Repair*. New York: Plenum Press, pp 275–308, 1996.
32. Villiger PM, Kusari AB, Ten Dijke P, Lotz M: IL-1 beta and IL-6 selectively induce transforming growth factor-beta isoforms in human articular chondrocytes. *J Immunol* 151:3337–3344, 1993.
33. Vodovotz Y, Chesler L, Chong H, Kim SJ, Simpson JT, DeGraff W, Cox GW, Roberts AB, Wink DA, Barcellos-Hoff MH: Regulation of transforming growth factor-β1 by nitric oxide. *Cancer Res* 59:2142–2149, 1999.
34. Luckhart S, Crampton AL, Zamora R, Lieber MJ, Dos Santos PC, Peterson TML, Emmith N, Lim J, Wink DA, Vodovotz Y: Mammalian transforming growth factor-β1 activated after ingestion by *Anopheles stephensi* modulates mosquito immunity. *Infect Immun* 71:3000–3009, 2003.
35. Nathan CF, Hibbs JB Jr: Role of nitric oxide synthesis in macrophage antimicrobial activity. *Curr Opin Immunol* 3:65–70, 1991.
36. Johnson ML, Billiar TR: Roles of nitric oxide in surgical infection and sepsis. *World J Surg* 22:187–196, 1998.
37. Babior BM: Phagocytes and oxidative stress. *Am J Med* 109:33–44, 2000.
38. Jaeschke H, Smith CW: Mechanisms of neutrophil-induced parenchymal cell injury. *J Leukoc Biol* 61:647–653, 1997.
39. Harbrecht BG, Billiar TR, Stadler J, Demetris AJ, Ochoa JB, Curran RD, Simmons RL: Nitric oxide synthesis serves to reduce hepatic damage during acute murine endotoxemia. *Crit Care Med* 20:1568–1574, 1992.
40. Florquin S, Amraoui Z, Dubois C, Decuyper J, Goldman M: The protective role of endogenously synthesized nitric oxide in staphylococcal enterotoxin B-induced shock in mice. *J Exp Med* 180:1153–1158, 1994.
41. Park J-H, Chang S-H, Lee K-M, Shin S-H: Protective effect of nitric oxide in an endotoxin-induced septic shock. *Am J Surg* 171:340–345, 1996.
42. Hack CE, Zeerleder S: The endothelium in sepsis: source of and a target for inflammation. *Crit Care Med* 29:S21–S27, 2001.
43. Beutler B: Endotoxin, toll-like receptor 4, and the afferent limb of innate immunity. *Curr Opin Microbiol* 3:23–28, 2000.
44. Ruiter DJ, van der Meulen J, Brouwer A, Hummel MJ, Mauw BJ, van der Ploeg JC, Wisse E: Uptake by liver cells of endotoxin following its intravenous injection. *Lab Invest* 45:38–45, 1981.
45. Maitra SK, Rachmilewitz D, Eberle D, Kaplowitz N: The hepatocellular uptake and biliary excretion of endotoxin in the rat. *Hepatology* 1:401–407, 1981.
46. Djeu JY, Serbousek D, Blanchard DK: Release of tumor necrosis factor by human polymorphonuclear leukocytes. *Blood* 76:1405–1409, 1990.
47. Romani L, Mencacci A, Cenci E, Spaccapelo R, Del Sero G, Nicoletti I, Trinchieri G, Bistoni F, Puccetti P: Neutrophil production of IL-12 and IL-10 in candidiasis and efficacy of IL-12 therapy in neutropenic mice. *J Immunol* 158:5349–5356, 1997.
48. Koller M, Clasbrummel B, Kollig E, Hahn MP, Muhr G: Major injury induces increased production of interleukin-10 in human granulocyte fractions. *Langenbecks Arch Surg* 383:460–465, 1998.
49. Glowacka E, Banasik M, Lewkowicz P, Tchorzewski H: The effect of LPS on neutrophils from patients with high risk of type 1 diabetes mellitus in relation to IL-8, IL-10 and IL-12 production and apoptosis in vitro. *Scand J Immunol* 55:210–217, 2002.
50. Cavaillon JM: Cytokines and macrophages. *Biomed Pharmacother* 48:445–453, 1994.
51. Bogdan C: Nitric oxide and the immune response. *Nat Immunol* 2:907–916, 2001.
52. Rees DD, Cunha FQ, Assreuy J, Herman AG, Moncada S: Sequential induction of nitric oxide synthase by *Corynebacterium parvum* in different organs of the mouse. *Br J Pharmacol* 114:689–693, 1995.
53. Santak B, Radermacher P, Iber T, Adler J, Wachter U, Vassilev D, Georgieff M, Vogt J: In vivo quantification of endotoxin-induced nitric oxide production in pigs from $Na^{15}NO_3$-infusion. *Br J Pharmacol* 122:1605–1610, 1997.
54. Bogdan C, Vodovotz Y, Nathan CF: Macrophage deactivation by interleukin 10. *J Exp Med* 174:1549–1555, 1991.
55. de Waal Malefyt R, Abrams J, Bennett B, Figdor CG, De Vries JE: Interleukin 10 (IL-10) inhibits cytokine synthesis by human monocytes: an autoregulatory role of IL-10 produced by monocytes. *J Exp Med* 174:1209–1220, 1991.
56. Aderka D, Le JM, Vilcek J: IL-6 inhibits lipopolysaccharide-induced tumor necrosis factor production in cultured human monocytes, U937 cells, and in mice. *J Immunol* 143:3517–3523, 1989.
57. Opal SM, DePalo VA: Anti-inflammatory cytokines. *Chest* 117:1162–1172, 2000.
58. Chong H, Vodovotz Y, Cox GW, Barcellos-Hoff MH: Immunocytochemical detection of latent TGF-β activation in cultured macrophages. *J Cell Physiol* 178:275–283, 1999.
59. Musso T, Espinoza-Delgado I, Pulkki K, Gusella GL, Longo DL, Varesio L: Transforming growth factor β downregulates interleukin-1 (IL- 1)-induced IL-6 production by human monocytes. *Blood* 76:2466–2469, 1990.
60. Maeda H, Kuwahara H, Ichimura Y, Ohtsuki M, Kurakata S, Shiraishi A: TGF-β enhances macrophage ability to produce IL-10 in normal and tumor-bearing mice. *J Immunol* 155:4926–4932, 1995.
61. Reibman J, Meixler S, Lee TC, Gold LI, Cronstein BN, Haines KA, Kolasinski SL, Weissmann G: Transforming growth factor beta 1, a potent chemoattractant for human neutrophils, bypasses classic signal-transduction pathways. *Proc Natl Acad Sci USA* 88:6805–6809, 1991.
62. Brandes ME, Mai UEH, Ohura K, Wahl SM: Type I transforming growth factor-β receptors on neutrophils mediate chemotaxis to transforming growth factor-β. *J Immunol* 147:1600–1606, 1991.
63. Drake WT, Issekutz AC: Transforming growth factor-β1 enhances polymorphonuclear leucocyte accumulation in dermal inflammation and transendothelial migration by a priming action. *Immunology* 78:197–204, 1993.
64. Wang H, Yang H, Czura CJ, Sama AE, Tracey KJ: HMGB1 as a late mediator of lethal systemic inflammation. *Am J Respir Crit Care Med* 164:1768–1773, 2001.
65. Tracey KJ: The inflammatory reflex. *Nature* 420:853–859, 2002.
66. Platzer C, Docke W, Volk H, Prosch S: Catecholamines trigger IL-10 release in acute systemic stress reaction by direct stimulation of its promoter/enhancer activity in monocytic cells. *J Neuroimmunol* 105:31–38, 2000.
67. Riese U, Brenner S, Docke WD, Prosch S, Reinke P, Oppert M, Volk HD, Platzer C: Catecholamines induce IL-10 release in patients suffering from acute myocardial infarction by transactivating its promoter in monocytic but not in T-cells. *Mol Cell Biochem* 212:45–50, 2000.
68. van der Poll T, Jansen J, Endert E, Sauerwein HP, van Deventer SJ: Noradrenaline inhibits lipopolysaccharide-induced tumor necrosis factor and interleukin 6 production in human whole blood. *Infect Immun* 62:2046–2050, 1994.
69. Molina PE: Noradrenergic inhibition of TNF upregulation in hemorrhagic shock. *Neuroimmunomodulation* 9:125–133, 2001.
70. Bernard AC, Mistry SK, Morris SM Jr, O'Brien WE, Tsuei BJ, Maley ME, Shirley LA, Kearney PA, Boulanger BR, Ochoa JB: Alterations in arginine metabolic enzymes in trauma. *Shock* 15:215–219, 2001.
71. Ochoa JB, Udekwu AO, Billiar TR, Curran RD, Cerra FB, Simmons RL, Peitzman AB: Nitrogen oxide levels in patients after trauma and during sepsis. *Ann Surg* 214:621–626, 1991.
72. Jacob TD, Ochoa JB, Udekwu AO, Wilkinson J, Murray T, Billiar TR, Simmons RL, Marion DW, Peitzman AB: Nitric oxide production is inhibited in trauma patients. *J Trauma* 35:590–596, 1993.

73. Myers PR, Wright TF, Tanner MA, Adams HR: EDRF and nitric oxide production in cultured endothelial cells: direct inhibition by *E. coli* endotoxin. *Am J Physiol Heart Circ Physiol* 31:H710–H718, 1992.
74. Parker JL, Myers PR, Zhong Q, Kim K, Adams HR: Inhibition of endothelium-dependent vasodilation by *Escherichia coli* endotoxemia. *Shock* 2:451–458, 1994.
75. Lu J-L, Schmiege LM, Kuo L, Liao JC: Downregulation of endothelial constitutive nitric oxide synthase expression by lipopolysaccharide. *Biochem Biophys Res Commun* 225:1–5, 1996.
76. Jones JJ, Sturek M, Adams HR, Parker JL: Endotoxin impairs agonist-stimulated intracellular free calcium (Ca(i)) responses in freshly dispersed aortic endothelial cells. *Shock* 15:386–391, 2001.
77. Buchman TG, Cobb JP, Lapedes AS, Kepler TB: Complex systems analysis: a tool for shock research. *Shock* 16:248–251, 2001.
78. Tjardes T, Neugebauer E: Sepsis research in the next millennium: concentrate on the software rather than the hardware. *Shock* 17:1–8, 2002.
79. Vodovotz Y, Clermont G, Chow C, An G: Mathematical models of the acute inflammatory response. *Curr Opin Crit Care* 10:383–390, 2004.
80. Butenas S, Mann KG: Blood coagulation. *Biochemistry (Mosc)* 67:3–12, 2002.
81. Neugebauer EA, Willy C, Sauerland S: Complexity and non-linearity in shock research: reductionism or synthesis? *Shock* 16:252–258, 2001.
82. Edelstein-Keshet L: *Mathematical Models in Biology.* New York: Random House, 1988.
83. An G: Agent-based computer simulation and SIRS: building a bridge between basic science and clinical trials. *Shock* 16:266–273, 2001.
84. An G: *In-silico* experiments of existing and hypothetical cytokine-directed clinical trials using agent based modeling. *Crit Care Med* 32:2050–2060, 2004.
85. Rangel-Frausto MS, Pittet D, Costigan M, Hwang T, Davis CS, Wenzel RP: The natural history of the systemic inflammatory response syndrome (SIRS). A prospective study. *JAMA* 273:117–123, 1995.
86. Sands KE, Bates DW, Lanken PN, Graman PS, Hibberd PL, Kahn KL, Parsonnet J, Panzer R, Orav EJ, Snydman DR: Epidemiology of sepsis syndrome in 8 academic medical centers. Academic Medical Center Consortium Sepsis Project Working Group. *JAMA* 278:234–240, 1997.
87. Clermont G, Angus DC: Severity scoring systems in the modern intensive care unit. *Ann Acad Med Singapore* 27:397–403, 1998.
88. Rosenbloom AJ, Pinsky MR, Bryant JL, Shin A, Tran T, Whiteside T: Leukocyte activation in the peripheral blood of patients with cirrhosis of the liver and SIRS. Correlation with serum interleukin-6 levels and organ dysfunction. *JAMA* 274:58–65, 1995.
89. Chang RW, Bihari DJ: Outcome prediction for the individual patient in the ICU. *Unfallchirurg* 97:199–204, 1994.
90. Opal SM, Fisher CJ Jr, Dhainaut JF, Vincent JL, Brase R, Lowry SF, Sadoff JC, Slotman GJ, Levy H, Balk RA, Shelly MP, Pribble JP, LaBrecque JF, Lookabaugh J, Donovan H, Dubin H, Baughman R, Norman J, DeMaria E, Matzel K, Abraham E, Seneff M: Confirmatory interleukin-1 receptor antagonist trial in severe sepsis: a phase III, randomized, double-blind, placebo-controlled, multicenter trial. *Crit Care Med* 25:1115–1124, 1997.
91. van der Poll T, van Deventer SJ: The role of interleukin 6 in endotoxin-induced inflammatory responses. *Prog Clin Biol Res* 397:365–377, 1998.
92. Lenczowski MJ, Van Dam AM, Poole S, Larrick JW, Tilders FJ: Role of circulating endotoxin and interleukin-6 in the ACTH and corticosterone response to intraperitoneal LPS. *Am J Physiol* 273:R1870–R1877, 1997.
93. Amiot F, Fitting C, Tracey KJ, Cavaillon JM, Dautry F: Lipopolysaccharide-induced cytokine cascade and lethality in LT alpha/TNF alpha-deficient mice. *Mol Med* 3:864–875, 1997.
94. Marino MW, Dunn A, Grail D, Inglese M, Noguchi Y, Richards E, Jungbluth A, Wada H, Moore M, Williamson B, Basu S, Old LJ: Characterization of tumor necrosis factor-deficient mice. *Proc Natl Acad Sci USA* 94:8093–8098, 1997.
95. Peschon JJ, Torrance DS, Stocking KL, Glaccum MB, Otten C, Willis CR, Charrier K, Morrissey PJ, Ware CB, Mohler KM: TNF receptor-deficient mice reveal divergent roles for p55 and p75 in several models of inflammation. *J Immunol* 160:943–952, 1998.
96. Smith JR, Hart PH, Coster DJ, Williams KA: Mice deficient in tumor necrosis factor receptors p55 and p75, interleukin-4, or inducible nitric oxide synthase are susceptible to endotoxin-induced uveitis. *Invest Ophthalmol Vis Sci* 39:658–661, 1998.
97. Pfeffer K, Matsuyama T, Kundig TM, Wakeham A, Kishihara K, Shahinian A, Wiegmann K, Ohashi PS, Kronke M, Mak TW: Mice deficient for the 55 kd tumor necrosis factor receptor are resistant to endotoxic shock, yet succumb to *L. monocytogenes* infection. *Cell* 73:457–467, 1993.
98. Bluethmann H, Rothe J, Schultze N, Tkachuk M, Koebel P: Establishment of the role of IL-6 and TNF receptor 1 using gene knockout mice. *J Leukoc Biol* 56:565–570, 1994.
99. Cuzzocrea S, De Sarro G, Costantino G, Ciliberto G, Mazzon E, De Sarro A, Caputi AP: IL-6 knock-out mice exhibit resistance to splanchnic artery occlusion shock. *J Leukoc Biol* 66:471–480, 1999.
100. LeBlanc RA, Pesnicak L, Cabral ES, Godleski M, Straus SE: Lack of interleukin-6 (IL-6) enhances susceptibility to infection but does not alter latency or reactivation of herpes simplex virus type 1 in IL-6 knockout mice. *J Virol* 73:8145–8151, 1999.
101. Manfredi B, Sacerdote P, Gaspani L, Poli V, Panerai AE: IL-6 knock-out mice show modified basal immune functions, but normal immune responses to stress. *Brain Behav Immun* 12:201–211, 1998.
102. Wang Q, Fang CH, Hasselgren PO: Intestinal permeability is reduced and IL-10 levels are increased in septic IL-6 knockout mice. *Am J Physiol Regul Integr Comp Physiol* 281:R1013–R1023, 2001.
103. Fattori E, Cappelletti M, Costa P, Sellitto C, Cantoni L, Carelli M, Faggioni R, Fantuzzi G, Ghezzi P, Poli V: Defective inflammatory response in interleukin 6-deficient mice. *J Exp Med* 180:1243–1250, 1994.
104. Khalil A, Tullus K, Bartfai T, Bakhiet M, Jaremko G, Brauner A: Renal cytokine responses in acute *Escherichia coli* pyelonephritis in IL- 6-deficient mice. *Clin Exp Immunol* 122:200–206, 2000.
105. Kopf M, Baumann H, Freer G, Freudenberg M, Lamers M, Kishimoto T, Zinkernagel R, Bluethmann H, Kohler G: Impaired immune and acute-phase responses in interleukin-6-deficient mice. *Nature* 368:339–342, 1994.
106. van der Poll T, Keogh CV, Guirao X, Buurman WA, Kopf M, Lowry SF: Interleukin-6 gene-deficient mice show impaired defense against pneumococcal pneumonia. *J Infect Dis* 176:439–444, 1997.
107. Lush CW, Cepinskas G, Sibbald WJ, Kvietys PR: Endothelial E- and P-selectin expression in iNOS- deficient mice exposed to polymicrobial sepsis. *Am J Physiol Gastrointest Liver Physiol* 280:G291–G297, 2001.
108. Hoit BD: Two faces of nitric oxide: lessons learned from the NOS2 knockout. *Circ Res* 89:289–291, 2001.
109. Cuzzocrea S, Mazzon E, Dugo L, Barbera A, Centorrino T, Ciccolo A, Fonti MT, Caputi AP: Inducible nitric oxide synthase knockout mice exhibit resistance to the multiple organ failure induced by zymosan. *Shock* 16:51–58, 2001.
110. Hickey MJ, Sharkey KA, Sihota EG, Reinhardt PH, MacMicking JD, Nathan C, Kubes P: Inducible nitric oxide synthase-deficient mice have enhanced leukocyte- endothelium interactions in endotoxemia. *FASEB J* 11:955–964, 1997.
111. Huang PL: Lessons learned from nitric oxide synthase knockout animals. *Semin Perinatol* 24:87–90, 2000.
112. Laubach VE, Foley PL, Shockey KS, Tribble CG, Kron IL: Protective roles of nitric oxide and testosterone in endotoxemia: evidence from NOS-2-deficient mice. *Am J Physiol* 275:H2211–H2218, 1998.
113. Mashimo H, Goyal RK: Lessons from genetically engineered animal models. IV. Nitric oxide synthase gene knockout mice. *Am J Physiol* 277:G745–G750, 1999.
114. Nicholson SC, Grobmyer SR, Shiloh MU, Brause JE, Potter S, MacMicking JD, Dinauer MC, Nathan CF: Lethality of endotoxin in mice genetically deficient in the respiratory burst oxidase, inducible nitric oxide synthase, or both. *Shock* 11:253–258, 1999.
115. Suzuki Y, Deitch EA, Mishima S, Lu Q, Xu D: Inducible nitric oxide synthase gene knockout mice have increased resistance to gut injury and bacterial translocation after an intestinal ischemia-reperfusion injury. *Crit Care Med* 28:3692–3696, 2000.
116. Molina PE: Opiate modulation of hemodynamic, hormonal, and cytokine responses to hemorrhage. *Shock* 15:471–478, 2001.
117. Bergmann M, Sautner T: Immunomodulatory effects of vasoactive catecholamines. *Wien Klin Wochenschr* 114:752–761, 2002.
118. Elenkov IJ, Wilder RL, Chrousos GP, Vizi ES: The sympathetic nerve—an integrative interface between two supersystems: the brain and the immune system. *Pharmacol Rev* 52:595–638, 2000.
119. Zinyama RB, Bancroft GJ, Sigola LB: Adrenaline suppression of the macrophage nitric oxide response to lipopolysaccharide is associated with differential regulation of tumour necrosis factor-alpha and interleukin-10. *Immunology* 104:439–446, 2001.

APPENDIX

Below are the ordinary differential equations of the model. The equations represent the dynamics of circulating or systemic levels of immune cells, cytokines, and molecules. Equations were derived from ''influence diagrams'' constructed from literature reports. We provide an example of such a diagram in Figure A1. Every arrow is linked to specific literature references hosted in a citation manager supporting the existence and occasionally providing quantitative information regarding the

process represented by this particular arrow. In addition, are two systemic variables representing blood pressure and tissue damage/dysfunction. The effect of trauma is expressed as an exponential decay of influence after an initial insult. It represents possible released cellular material that can trigger inflammation. The function fB(B) is phenomenological and represents the stimulatory effect of a decrease in blood pressure on triggering a stress response. This occurs in a variety of ways, and we are currently examining how to model it more exactly as part of ongoing projects in larger animals. Small deviations from normality probably are of little consequence, whereas larger deviations are proportionally more harmful (and rapidly so) as the ability of the organism to compensate decreases. This is what explains the phenomenological fourth-power exponent. For numerical ease, the variables of the equations are defined in abstract units of concentration. The actual units are restored with a linear scaling factor when compared to experimental data. The time unit is fixed at hours. The differential equations were solved numerically using the XPPAUT freeware written by Dr. G. B. Ermentrout (University of Pittsburgh, Department of Mathematics; *www.math.pitt.edu/~phase*) as well as proprietary software of Immunetrics, Inc. The fitting process included quantitative data, but the overall behavior of the model had also to be compatible with various qualitative scenarios extracted from the literature. These scenarios are listed in Table 2. Failure to comply with any of those qualitative behaviors resulted in discarding a given model.

Equations

$$M_A' = \left[\left(k_{MLPS}\frac{LPS(t)^2}{1+(LPS(t)/x_{MLPS})^2} + k_{MD}\frac{D^4}{x_{MD}^4+D^4}\right) \times\left(\frac{TNF^2}{x_{MTNF}^2+TNF^2} + k_{M6}\frac{IL6^2}{x_{M6}^2+IL6^2}\right) + k_{MTR}TR(t) + k_{MB}f_B(B)\right] \frac{1}{1+((IL10+CA)/x_{M10})^2}M_R - k_{MA}M_A$$

$$N_R' = -\left(k_{NLPS}\frac{LPS(t)}{1+LPS(t)/x_{NLPS}} + k_{NTNF}\frac{TNF}{1+TNF/x_{NTNF}} + k_{N6}\frac{IL6^2}{1+(IL6/x_{N6})^2} + k_{ND}\frac{D^2}{1+(D/x_{ND})^2} + k_{NB}f_B(B) + k_{NTR}TR(t)\right) \times\frac{1}{1+((IL10+CA)/x_{N10})^2}N_R - k_{NR}(N_R - S_N)$$

$$M_R' = -\left[\left(k_{MLPS}\frac{LPS(t)^2}{1+(LPS(t)/x_{MLPS})^2} + k_{MD}\frac{D^4}{x_{MD}^4+D^4}\right) \times\left(\frac{TNF^2}{x_{MTNF}^2+TNF^2} + k_{M6}\frac{IL6^2}{x_{M6}^2+IL6^2}\right) + k_{MTR}TR(t) + k_{MB}f_B(B)\right] \frac{1}{1+((IL10+CA)/x_{M10})^2}M_R - k_{MR}(M_R - S_M)$$

$$N_A' = \left(k_{NLPS}\frac{LPS(t)}{1+LPS(t)/x_{NLPS}} + k_{NTNF}\frac{TNF}{1+TNF/x_{NTNF}} + k_{N6}\frac{IL6^2}{1+(IL6/x_{N6})^2} + k_{ND}\frac{D^2}{1+(D/x_{ND})^2} + k_{NB}f_B(B) + k_{NTR}TR(t)\right) \times\frac{1}{1+((IL10+CA)/x_{N10})^2}N_R - k_{NA}N_A$$

$$iNOSd' = (k_{INOSN}N_A + k_{INOSM}M_A + k_{INOSEC} \left(\frac{TNF^2}{1+(TNF/x_{INOSTNF})^2} + k_{INOS6}\frac{IL6^2}{1+(IL6/x_{INOS6})^2}\right)) \times\frac{1}{1+(IL10/x_{INOS10})^2}\frac{1}{1+(NO/x_{iNOSNO})^4} - k_{INOSd}iNOSd$$

$$iNOS' = k_{iNOS}(iNOSd - iNOS),$$

$$eNOS' = k_{ENOSEC}\frac{1}{1+TNF/x_{ENOSTNF}}\frac{1}{1+LPS(t)/x_{ENOSLPS}}\frac{1}{1+(TR(t)/x_{ENOSTR})^4} - k_{ENOS}eNOS$$

$$NO_3' = k_{NO3}(NO - NO_3)$$

$$TNF' = (k_{TNFN}N_A + k_{TNFN}M_A) \frac{1}{1+((IL10+CA)/x_{TNF10})^2}\frac{IL6}{1+(IL6/x_{TNF6})^3} - k_{TNF}TNF$$

$$IL6' = \left(k_{6N}N_A + M_A\right)\left(k_{6M} + k_{6TNF}\frac{TNF^2}{x_{6TNF}^2+TNF^2} + k_{6NO}\frac{NO^2}{x_{6NO}^2+NO^2}\right) \frac{1}{1+((CA+IL10)/x_{610})^2} + k_6(S_6 - IL6)$$

$$IL12' = k_{12M}M_A\frac{1}{1+(IL10/x_{1210})^2} - k_{12}IL12$$

$$CA' = k_{CATR}A(t) - k_{CA}CA$$

$$IL10' = (k_{10N}N_A + M_A(1 + k_{10A}A(t)) \left(k_{10MR} + k_{10TNF}\frac{TNF^4}{x_{10TNF}^4+TNF^4} + k_{106}\frac{IL6^4}{x_{106}^4+IL6^4}\right) \left((1 - k_{10R})\frac{1}{1+(IL12/x_{1012})^4} + k_{10R}\right) - k_{10}(IL10 - S_{10})$$

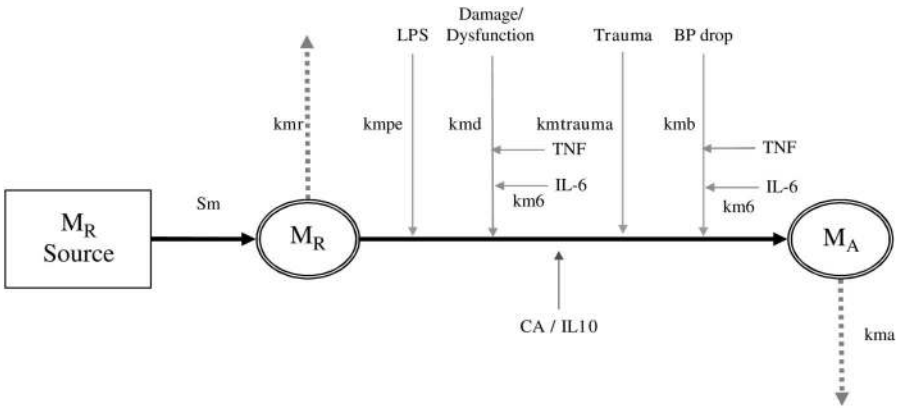

FIG. A1. **A simplified version of macrophage dynamics**. In the model used herein, resting macrophages (M_R) are activated by a number of physiologic processes, including endotoxin (PE), damage/dysfunction, trauma and hypotension (blood pressure [BP] drop). This recruitment process can be upregulated (green lines) in the presence of tumor necrosis factor TNF and interleukin (IL)-6, whereas IL-10 and other antiinflammatory (CA) molecules downregulate (red line) these activating influences. Both resting and activated macrophages (M_A) "die" at their respective rates (gray dotted line). Each process is supported by a literature search.

$$B' = k_B\left(\frac{B_0 - Hem(t)}{1 + k_{BNO}(NO - x_{BNO})} - B\right)$$

$$D' = \left(k_{DB}f_B(B) + k_{D6}\frac{IL6^4}{x_{D6}^4 + IL6^4} + k_{DTR}TR(t)\right)\frac{1}{x_{DNO}^2 + NO^2} - k_D D$$

where

$$NO = iNOS(1 + k_{NOMN}(M_A + N_A)) + eNOS$$

$$LPS(t) = LPS(0)\exp(-k_{LPS}t),$$
$$TR(t) = TR_{ON}\exp(-(t - t_{TR})^2/x_{TR}^2),$$
$$A(t) = A_{ON}\exp(-(t - t_A)^2/x_A^2)$$

$$f_B(B) = H(B_0 - B)(B_0 - B)^4,$$
$$Hem(t) = (B_0 - B(0))H(t_{HRES} - t),$$
$$H(x) = \begin{cases} 1, x > 0. \\ 0, x < 0 \end{cases}$$

Model Parameters

Model parameters are divided into several categories: initial conditions, source terms, rate constants, and saturation constants (Table A1). The initial conditions determine different experimental paradigms. For endotoxemia: $LPS(0) = 3$, 6, or 12, $TR_{ON} = 0$, $A_{ON}(0) = 0$, $B(0) = 1$; for trauma: $LPS(0) = 0$, $TR_{ON} = 1$, $A_{ON} = 1$, $B(0) = 1$; for hemorrhage: $LPS(0) = 0$, $TR_{ON} = 1$, $A_{ON} = 1$, $B(0) = 0.25$.

Units

The time unit is fixed at hours. The variables are all in relative units. To match the data we use conversion factors of 35,000, 17,000, 8,000, and 1,000, respectively, to convert the arbitrary units of TNF, IL-6, IL-10, and NO_3 into true concentrations (pg/L). The variable A is a simple representation of autonomic outflow. Epinephrine and other biogenic amines released at the time of acute stressor such as hemorrhage are well known to briefly stimulate IL-10 and to a lesser degree IL-6, IL-12, and other modulators of immunity (67, 116–119). The exponential decay was inserted to mimic the empirical observation of a similar decay in circulating catecholamines and to reflect the brevity of their biological action on immune cells.

Statistical Complement

Examination of the data shows high heteroskedasticity for observations obtained in different animals. A closer study of the scatter shows a power law relationship between the standard deviation and the mean of the analyte response, closely approximating $\sigma = 1.57\mu^{0.76}$, where σ is the standard deviation and μ is the mean. A consequence of this relationship is that, in addition to assessing the model by using the individual data points directly, we can also compare the model to the mean responses, keeping in mind the fact that the observed error in response is proportional to the mean response itself to a power of approximately three-quarters.

A detailed analysis of fit yields the following correlation coefficients (four analytes—IL-10, IL-6, NO, and TNF—in four scenarios—LPS doses at 3 mg/kg, 6 mg/kg, and 12 mg/kg, shock, and surgical trauma): IL10, 0.69 0.57 0.85 0.58 0.48; IL6, 0.78 0.98 0.82 0.54 0.72; NO, 0.70 0.84 0.71 0.35 0.17; TNF, 0.38 0.87 0.34 0.48 0.49. Therefore, although the fit overall is good, $P < 0.0001$, some curves are not described as well by the model.

TABLE A1. **Model parameters**

Initial conditions and source terms					
S_M = 1.0	t_{HRES} = 2.5	$M_R(0)$ = 1	iNOS(0) = 0	TNF(0) = 0	B0 = 1.0
S_N = 1.0	t_{TR} = 1.86	$M_A(0)$ = 0	iNOS3(0) = 0	IL6(0) = 0.001	IL12(0) = 0
S_6 = 0.001	x_{TR} = 0.6785	$N_R(0)$ = 1	eNOS(0) = .05	IL10(0) = 0.01	x_A = 1.1636
S_{10} = 0.01	t_A = 2.0138	$N_A(0)$ = 0	$NO_3(0)$ = 0	CA(0) = 0	D(0) = 0
Rate constants					
k_{LPS} = 1.0	k_{NTNF} = 0.2	k_{INOSN} = 1.5	k_{NO3} = 0.46	K_6 = 0.7	k_{CA} = 0.1
k_{MLPS} = 1.01	k_{N6} = 0.557	k_{INOSM} = 0.1	k_{NOMA} = 2.0	k_{6N} = 0.2	k_{CATR} = 0.16
k_{MTR} = 0.04	k_{NB} = 0.1	k_{INOSEC} = 0.1	k_{TNFN} = 2.97	k_{10MA} = 0.1	k_{12M} = 0.303
k_{M6} = 0.1	k_{ND} = 0.05	k_{INOS6} = 2.0	k_{TNFM} = 0.1	k_{10N} = 0.1	k_{12} = 0.05
k_{MB} = 0.0495	k_{NTR} = 0.02	k_{INOSd} = 0.05	k_{TNF} = 1.4	k_{10A} = 62.87	k_B = 4
k_{MR} = 0.05	k_{NTGF} = 0.1	k_{INOS} = 0.101	k_{6M} = 3.03	k_{10TNF} = 1.485	k_{BNO} = 0.2
k_{MA} = 0.2	k_{NR} = 0.05	k_{ENOS} = 4.0	k_{6TNF} = 1.0	k_{106} = 0.051	k_{DB} = 0.02
k_{MANO} = 0.2	k_{NNO} = 0.4	k_{ENOSEC} = 0.05	k_{62} = 3.4	k_{10} = 0.35	k_{D6} = 0.3
k_{NLPS} = 0.15	k_{NA} = 0.5	k_N = 0.5	k_{6NO} = 2.97	k_{10R} = 0.1	k_D = 0.05
					k_{DTR} = 0.05
Saturation constants					
x_{MLPS} = 10	x_{NLPS} = 15.0	x_{INOS10} = 0.1	x_{ENOSTR} = 0.1	x_{6NO} = 0.4	x_{1210} = 0.2525
x_{MD} = 1.0	x_{NTNF} = 2.0	$x_{INOSTNF}$ = 0.05	x_{TNF6} = 0.059	x_{10TNF} = 0.05	x_{BNO} = 0.05
x_{MTNF} = 0.4	x_{N6} = 1.0	x_{INOS6} = 0.1	x_{TNF10} = 0.079	x_{1012} = 0.049	x_{D6} = 0.25
x_{M6} = 1.0	x_{ND} = 0.4	x_{INOSNO} = 0.3	x_{610} = 0.1782	x_{106} = 0.08	x_{DNO} = 0.4
x_{M10} = 0.297	x_{N10} = 0.2	$x_{ENOSTNF}$ = 0.4	x_{6TNF} = 0.1	x_{12TNF} = 0.2	
x_{MCA} = 0.9	x_{NNO} = 0.5	$x_{ENOSLPS}$ = 1.015	x_{66} = 0.2277	x_{126} = 0.2	